# Reconstruction of uranium and plutonium isotopic signatures in sediment accumulated in the Mano Dam reservoir, Japan, before and after the Fukushima nuclear accident

Hugo Jaegler, Fabien Pointurier, Silvia Diez-Fernández, Alkiviadis Gourgiotis, Hélène Isnard, Seiji Hayashi, Hideki Tsuji, Yuichi Onda, Amelie Hubert, J. Patrick Laceby, et al.

# Reconstruction of uranium and plutonium isotopic signatures in sediment accumulated in the Mano Dam reservoir, Japan, before and after the Fukushima accident

Hugo Jaegler[1], Fabien Pointurier[2], Silvia Diez-Fernández[3], Alkiviadis Gourgiotis[4], Hélène Isnard[3], Seiji Hayashi[5], Hideki Tsuji[5], Yuichi Onda[6], Amélie Hubert[2], J. Patrick Laceby[1,7] & Olivier Evrard[1]*

**Affiliations:**

[1]Laboratoire des Sciences du Climat et de l'Environnement, LSCE/IPSL, UMR 8212 (CEA-CNRS-UVSQ), Université Paris-Saclay, F-91198 Gif-sur-Yvette Cedex, France

[2]CEA, DAM, DIF, F-91297 Arpajon, France

[3] Den – Service d'Etudes Analytiques et de Réactivité des Surfaces (SEARS), CEA, Université Paris-Saclay, F-91191, Gif sur Yvette, France

[4]Institut de Radioprotection et de Sûreté Nucléaire - PSE/ENV - SEDRE/LELI BP 17, Fontenay-aux-Roses, 92262, France

[5]National Institute for Environmental Science, Fukushima Branch, 10-2 Fukasaku, Miharu, Tamura, Fukushima, 963-7700 Japan

[6]Center for Research in Isotopes and Environmental Dynamics (CRIED), University of Tsukuba, Tsukuba, Japan

[7]Environmental Monitoring and Science Division, Alberta Environment and Parks, 3115 – 12 Street NE Calgary, Alberta, Canada

(*) Corresponding author (email address: olivier.evrard@lsce.ipsl.fr).

## Abstract

The Fukushima Dai-ichi Nuclear Power Plant (FDNPP) accident in Japan resulted in a major release of radionuclides into the environment. Compared to others elements, few studies have investigated the emission of actinides. Accordingly, this research investigates the Pu composition in soil samples collected in nearby paddy fields before and after the accident. Furthermore, the vertical distributions of Pu and U isotopic signatures, along with $^{137}Cs$ activities, were measured in a sediment core collected in 2015 in the Mano Dam reservoir, in the Fukushima Prefecture. These signatures were used to quantify changes in the relative contributions of the major actinide sources (global fallout or FDNPP derived fallout) in sediment deposited in the reservoir. The distinct peak observed for all Pu isotope ratios ($^{240}Pu/^{239}Pu$, $^{241}Pu/^{239}Pu$ and $^{242}Pu/^{239}Pu$) and for $^{137}Cs$ concentrations in the sediment core was attributed to the Fukushima fallout, and coincided with the maximum atomic contribution of only 4.8±1.0% of Pu from the FDNPP. Furthermore, $^{236}U/^{238}U$ ratios measured in the sediment core remained close to the global fallout signature indicating there was likely no U from the FDNPP accident in the sediment core. More research is required on the environmental dynamics of trace actinides in landscapes closer to the FDNPP where greater abundances of FDNPP-derived Pu and U would be anticipated.

## Abstract art

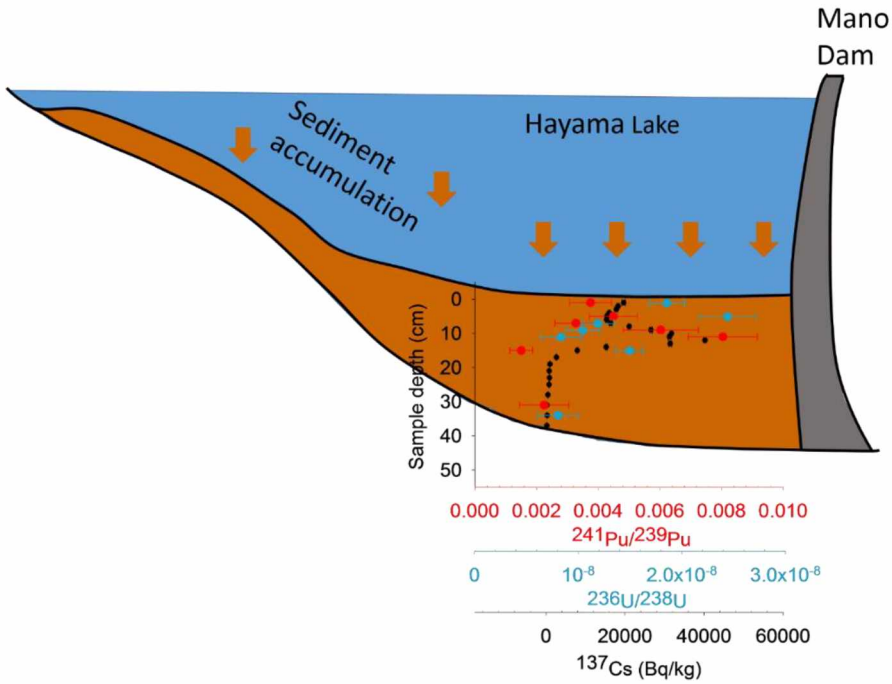


## Introduction

The 2011 Fukushima Dai-ichi Nuclear Power Plant (FDNPP) accident released significant volumes of radionuclides into the environment. In particular, various venting operations and explosions occurred at the FDNPP and triggered the release of volatile fission products ($^{131}$I, $^{132}$Te, $^{134}$Cs and $^{137}$Cs)(Schneider et al., 2017). Accordingly, numerous studies were conducted to investigate the distribution and the fate of the gamma-emitting isotopes, including radiocesium, after the accident(Buesseler et al., 2016; Cao et al., 2016; Tanaka et al., 2015; Yamamoto et al., 2012; Zheng et al., 2014). Erosion and remobilisation of particle-bound radiocesium contamination was investigated through field monitoring(Evrard et al., 2016; Yamashiki et al., 2014) and model simulations(Kitamura et al., 2016; Kitamura et al., 2014). These studies reported a rapid export of the particle-bound radioactive contamination by the coastal rivers to the Pacific Ocean, with the preferential remobilisation of fine sediment particles enriched in radiocesium. This process was shown to be

exacerbated during heavy typhoons, because of the strong hillslope-to-river sediment connectivity observed, particularly with paddy fields that were found to be one of the main sources of radiocesium shortly after the accident(Chartin et al., 2017; Laceby et al., 2016; Lepage et al., 2016). Importantly, dams and reservoirs were demonstrated to store significant quantities of contaminated sediment in the region and their management represents a significant challenge for the regional authorities(Chartin et al., 2013; Yamada et al., 2015).

Although radiocesium sources have been extensively researched, less information is available in the literature regarding the fate of other radionuclides such as U or Pu. Non-volatile Pu isotopes including $^{239}Pu$ ($T_{1/2}$=24,110 y, alpha-decay), $^{240}Pu$ ($T_{1/2}$=6,563 y, alpha-decay), $^{241}Pu$ ($T_{1/2}$=14.35 y, beta-decay) and $^{242}Pu$ ($T_{1/2}$=376,000 y, alpha-decay)(Evrard et al., 2014; Xu et al., 2016; Yamamoto et al., 2014; Zheng et al., 2012b) and U isotopes including $^{238}U$ ($T_{1/2}=4.469\times10^{9}$ y, alpha-decay), $^{235}U$ ($T_{1/2}=7.038\times10^{8}$ y, alpha-decay), $^{234}U$ ($T_{1/2}$=245,500 y, alpha-decay) and $^{236}U$ ($T_{1/2}=23.42\times10^{6}$ y, alpha-decay)(Sakaguchi et al., 2014; Schneider et al., 2017; Shinonaga et al., 2014; Yang et al., 2016), were also detected in environmental samples collected in the Fukushima Prefecture. These radionuclides may originate from two main sources: the global fallout associated with the nuclear atmospheric weapon tests(Yamamoto et al., 2014) and the FDNPP accident. Additionally, $^{238}U$, $^{235}U$ and $^{234}U$ isotopes are naturally present in the environment. As Pu ($^{240}Pu/^{239}Pu$, $^{241}Pu/^{239}Pu$ and $^{242}Pu/^{239}Pu$) and U ($^{236}U/^{238}U$) isotope ratios may vary significantly depending on their source(Muramatsu et al., 2003; Schneider et al., 2017), their precise measurement in sediment could provide powerful fingerprints for source identification. Accordingly, investigating the changes in the Pu and U signatures with depth in lacustrine sediment cores should provide information for reconstructing the changes in the respective contributions of these radionuclide sources in lacustrine sediment.

To the best of our knowledge, the analysis of Pu isotopes in continental sediment deposited in reservoirs following the FDNPP accident has been restricted to that of cores collected in the Lake Inba, located 200 km south of the FDNPP site (i.e. outside of the main radioactive plume)(Cao et al., 2017). Although the measured $^{134}Cs/^{137}Cs$ ratios indicated there was fallout from the FDNPP accident,

the $^{239+240}$Pu activity and the $^{240}$Pu/$^{239}$Pu ratio remained similar to the global fallout signature, suggesting that FDNPP-derived Pu did not reach the Lake Inba basin in significant quantities.

In this study, the global fallout signature was first refined for the study region through the analysis of soil samples collected before the accident. Soils collected after the accident were analysed to characterise the initial spatial pattern of Pu deposited in this area and to compare it with the well-documented $^{137}$Cs deposition pattern. Then, the vertical distribution of Pu and U isotope ratios was characterised in a sediment core. These distributions were compared to that of $^{137}$Cs concentrations measured in the core, and the contributions of the different sources of Pu in this region (global fallout vs. FDNPP) were quantified through the analysis of Pu isotope ratios. Implications regarding the fate and the geochemical behaviour of actinides in the catchments draining the main radioactive plume in the Fukushima Prefecture are then discussed.

## Materials and methods

### Soil and sediment sampling

In order to provide the local signature of the Pu global fallout in this region, four soil samples collected before the accident (in 2007 and in 2010, see Table S1) were first analysed. These samples were taken at two different locations in cultivated paddy fields (12 km to the south-west of the Mano Dam, see Figure 1) and at two different depths (ploughed and underlying layers). To characterise the initial deposition of FDNPP-derived Pu, soil samples collected shortly after the accident (in November 2011, November 2012 and April 2012, see Table S2) were also analysed. Soil samples were taken from a range of $^{137}$Cs fallout levels to be representative of potential FDNPP fallout (see Figure 1). Sampling methods are described elsewhere(Jaegler et al., 2018). In brief, soil samples are composed

of 10 soil scrape subsamples, taken with a plastic trowel, that were thoroughly homogenized prior to analyses.

A sediment core collected in Lake Hayama, which is located 39 km to the northwest of the FDNPP in the Mano River catchment, was analysed. This lake corresponds to the artificial Mano Dam reservoir, with an area of 1.75 $km^2$, a water volume of 36,200 $\times 10^3$ $m^3$ and a retention time of 0.48 year(Fukushima and Arai, 2014; Matsuda et al., 2015).

Researchers have investigated the radioactive contamination of sediment accumulated in this lake, although they restricted their analysis to radiocesium concentrations. Matsuda *et al.*(2015) measured the radiocesium concentration in bottom sediment and in lake water samples in 2012 and 2013, and they observed respective concentration decreases of 57% and 43% between the successive sampling campaigns. Huon *et al.(2018)* measured the vertical distribution of $^{137}Cs$ activities in four sediment cores sampled across the lake. Three of these four cores showed a distinct peak likely corresponding to the initial radiocesium wash-off and migration phase following the FDNPP accident. In the current study, one of these sediment cores (referred to as 'DD1') located in the downstream section of the lake and composed of fine sediment material(Huon et al., 2018) was selected to characterise variations of Pu and U isotope ratios with depth. More details on the core sampling and the radiocesium analyses are provided in Huon *et al.(2018)*. In brief, the sediment core was collected on April 24, 2015 (37°43'25.75"N, 140°49'49.84"E) using a gravity core sampler, under approximately 45 m of water. The sediment core was 37 cm long and was then divided into 1-cm increments from 0 to 15 cm depth, 2 cm from 15 to 25 cm depth and, finally, 3 cm from 25 to 37 cm depth. $^{137}Cs$ content was measured by gamma spectrometry in each subsample in order to investigate the distribution of $^{137}Cs$ in the core(Huon et al., 2018).

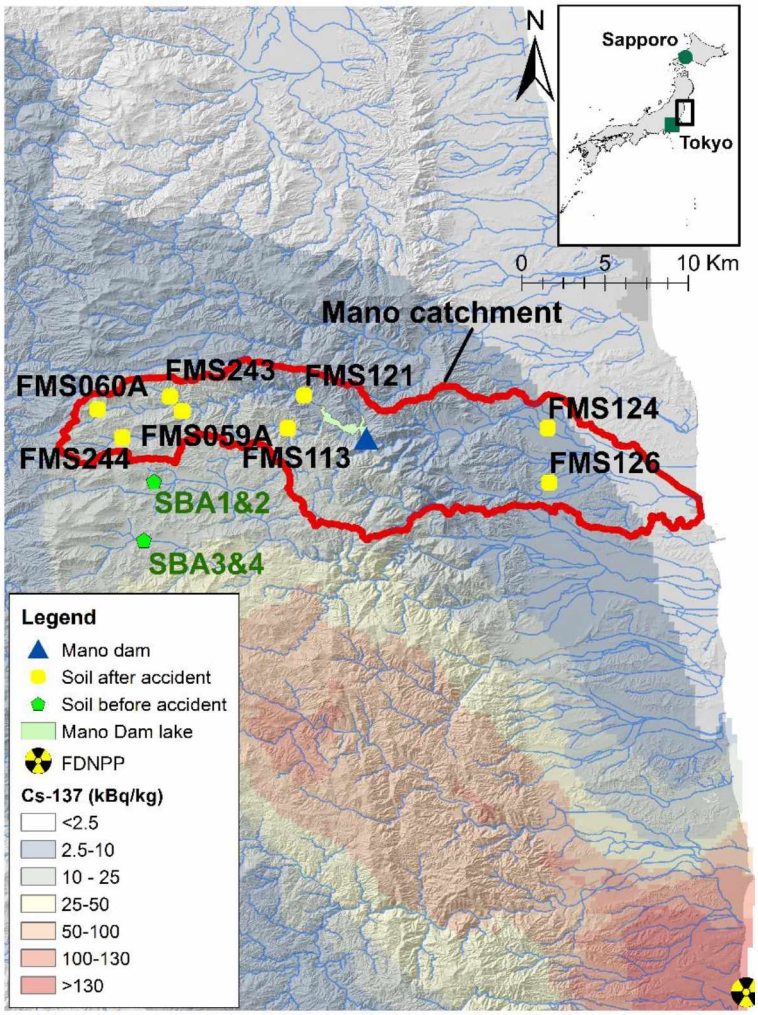


Figure 1: Location of the soil samples analysed in this current research in the Mano catchment delineated in red. The main radiocaesium contamination plume is also located in the background map derived from Chartin *et al.(2013)*.

## Chemical preparation and separation of plutonium and uranium

Core sections were grouped by pairs to provide sufficient material (~5 g) for the actinide analyses. Samples were placed in an electric furnace at 450 °C for ~15 h to decompose the organic matter. After cooling to room temperature, they were transferred in Savillex® PFA Teflon® beakers. ~100 fg of $^{244}$Pu (diluted solution prepared from the certified isotopic reference material IRMM-042a, Geel, Belgium) was added as an isotopic dilution tracer. Chemical blanks were spiked as well. Digestion of

142 the samples was carried out through several acid leaching steps. Only partial dissolution protocol was
143 performed as it was shown that this partial leaching was sufficient to dissolved actinide contained in
144 samples(Lee et al., 2005,Liao, 2008 #532,Jaegler, 2018 #970). Moreover, total dissolution required
145 use of concentrated HF acid, which is known to contain more impurities than concentrated HCl and
146 $HNO_3$ acid.

147 50 mL concentrated $HNO_3$, 50 mL aqua regia and 50 mL concentrated HCl. Between each leaching
148 step, the solutions were dried in a closed evaporation system (Evapoclean®, Analab, Hoenheim,
149 France) at 110 °C until complete dryness. This device allows evaporation in a closed medium to
150 prevent any lab contamination. Samples were then recovered with 2M HCl and filtrated with a
151 disposable 0.45 µm Nalgene filtering unit (Thermo Scientific, Rochester, NY, USA). Dissolved fractions
152 were transferred in clean Savillex® PFA Teflon® beakers and evaporated to dryness in closed media.
153 Samples were then recovered with 50 mL of concentrated $HNO_3$ and a few mg of $NaNO_2$ were added
154 to stabilize the (+IV) oxidation state of Pu and evaporated to dryness. Samples were finally recovered
155 with 30 mL of 8M $HNO_3$ before Pu separation on chromatographic columns. The first column was
156 composed of a Dowex AG1X8 anion-exchange resin filled with ~10 mL of 50-100 mesh AG1X8 resin
157 and ~10 mL of 100-200 mesh AG1X8 resin, conditioned with 8 M $HNO_3$. After loading the sample
158 onto the column, U was first eluted with 8M $HNO_3$. Then, Th was eliminated with 10 M HCl. Pu was
159 finally eluted with $NH_4I$ (1.5%) – 12 M HCl.

160 The same protocol was repeated twice on the Pu fraction with 2 mL Dowex AG1X4 anion-exchange
161 resin (100-200 mesh) to reduce as much as possible sample matrix elements, which can potentially
162 generate polyatomic (mainly $PbO_2^+$, $^{238}UH^+$) and isobaric ($^{241}Am^+$) interferences. After evaporation of
163 the eluate, samples were recovered and evaporated to dryness several times with concentrated
164 $HNO_3$ to eliminate chlorides. Finally, the last recovery was performed with 2% $HN0_3$ + 0.01M HF for
165 ICP-MS measurements. The two consecutive purifications of the Pu fraction with Dowex resins
166 allowed a complete elimination of Am(Trémillon, 1965). However, $PbO_2^+$ and $UH^+$ interferences
167 persisted during ICP-MS measurements and required raw data corrections. The U fraction collected

with the first Dowex AG1X8 was further purified with a second column of 2 mL UTEVA extraction resin (100 – 150 µm), conditioned with 4M $HNO_3$. U was directly eluted with 0.01M $HNO_3$. After evaporation to dryness of this eluted solution, the U fraction of samples was finally recovered with 2% $HNO_3$ for ICP-MS measurements. At least two chemical blanks were systematically prepared with sample treatments. The sample preparation and Pu and U separation protocol efficiency was confirm by analysing certified reference materials in a previous study (Jaegler et al., 2018).

**Plutonium measurements by mass-spectrometry**

Pu isotopic composition in the samples were measured with a Multi-Collector Inductively Coupled Plasma Mass Spectrometer (MC-ICP-MS) (Neptune Plus, Thermo Fisher Scientific Inc., Bremen, Germany) equipped with eight Faraday cups and five ion counters for the simultaneous detection of ion beams. All measurements were performed using Aridus II (Cetac) as introduction system, high-efficiency sampler and skimmer cones, reinforced pumping in the interface to enhance the sensitivity by a factor of ~10 (approximately $10^8$ counts/s per µg/L of $^{238}U$), compared to the standard configuration.

Two certified reference materials, IRMM 186 and IRMM 057 (both reference materials were provided by the Institute for Reference Materials and Measurements, Geel, Belgium), were measured on a regular basis throughout each analysis sequence and used to correct interferences and biases: instrumental mass fractionation, peak tailing at M+1 and M+2, and hydride formation (mainly $^{238}UH^+$) were determined. Lead polyatomic interferences ($PbO_2^+$) were corrected by measuring three pure mono-elemental solutions of Pb at the end of the procedure. Measurement of these standards in the chemical blanks shows that main lead interferences are instrumental induced (PbAr) rather than induced by the chemical protocol (PbCl). Moreover, as levels of interferences as similar in the blanks and in the sample, it shows that Pb is originating from the reagents added during radiochemical protocol and not contained in the sample. All these corrections were applied to a

193 solution of the Pu isotopic certified material CRM128 (NBL, US DOE) for verification. Finally, all Pu
194 compositions were corrected for tracer impurities according to the certificate of the isotopic
195 reference material IRMM-042a, decay-corrected to March 15, 2011 and for blank levels (average of
196 total Pu in the blanks: 3.4 ± 1.2 fg).

197

198 **Uranium measurements by mass spectrometry**

199

200 Precise $^{236}U$ measurements were performed twice in two different laboratories: at CEA/LANIE
201 ("Commissariat à l'Energie Atomique et aux Energies Alternatives/ Laboratoire de développement
202 Analytique Nucléaire, Isotopique, Elémentaire") and at IRSN/LELI ("Institut de Radioprotection et de
203 Sureté du Nucléaire / Laboratoire sur le devenir des pollutions des sites radioactifs") using two ICP-
204 MS/MS (Agilent 8800, Agilent Technologies, Tokyo, Japan) instruments well-suited for the
205 measurement of extremely low $^{236}U/^{238}U$ isotope ratios(Tanimizu et al., 2013; Yang et al., 2016). Two
206 analyses on each sample were conducted to provide more confidence in the results. The strategy
207 followed in both laboratories was based on the mass shift mode (through the detection of the oxide
208 form, $U^{16}O^{+}$) as described by Tanimizu *et al.* and Yang *et al.(2013; 2016)*. This strategy allowed for
209 reducing $^{238}U$ and $^{235}U$ peak tailing and hydride formation from $^{235}U$ at m/z=236 opening up the
210 possibility to measure very low $^{236}U/^{238}U$ isotope ratios. Owing to these strong interferences, the
211 measurement of very low $^{236}U/^{238}U$ ratios by MC-ICP-MS is limited.

212 Both laboratories are equipped with the same ICP-MS/MS instrument and used desolvating
213 introduction systems in order to increase sensitivity and to reduce the formation of hydrides.
214 However, desolvating devices and measurement procedures showed significant differences.

215 The LANIE laboratory used the Aridus (Cetac Technologies, Omaha, NE, USA) introduction system.
216 The $^{236}U/^{238}U$ in the samples was deduced through the measurement of $^{236}UO^{+}/^{235}UO^{+}$ using the
217 natural $^{238}U/^{235}U$ (137.88) ratio (as $^{238}U$ and $^{235}U$ are mostly originating from natural uranium).

$^{236}UO^{+}/^{235}UO^{+}$ ratio was corrected for hydride formation ($^{235}UOH^{+}/^{235}UO^{+}$) and for the chemical blanks. The instrumental mass fractionation was internally corrected using the $^{234}UO^{+}/^{235}UO^{+}$ ratios of the samples, compared with the $^{234}U/^{235}U$ isotope ratio also determined with another ICP-MS instrument.

The LELI laboratory used the Apex-HF (Elemental Scientific, Omaha, NE, USA) introduction system. In order to acquire signals only with the pulse counting mode during the analysis, the $^{236}UO^{+}/^{235}UO^{+}$ ratio was measured and the $^{236}U/^{238}U$ was deduced using the natural $^{238}U/^{235}U$ (137.88) ratio. Instrumental mass fractionation was corrected by a standard bracketing method using the measured $^{234}U/^{235}U$ ratio of an IRMM186 certified solution. A hydride correction factor was calculated using the $^{238}UOH^{+}/(^{235}UO^{+}\times 137.88)$ ratio and applied to the $^{236}U$ measurements to correct for the $^{235}UO^{+}$ hydride formation.

**Pu and U source term signatures**

Pu deposition on soils of this region may originate from two main sources: the global fallout and the FDNPP accident. Pu fuel isotopic compositions at the moment of the accident were estimated to be $0.373 \pm 0.044$ ($2\sigma$) for $^{240}Pu/^{239}Pu$, $0.1874 \pm 0.0081$ ($2\sigma$) for $^{241}Pu/^{239}Pu$, and $0.0637 \pm 0.0026$ ($2\sigma$) for $^{242}Pu/^{239}Pu$(Kirchner et al., 2012; Nishihara et al., 2012; Schwantes et al., 2012).

The global fallout signatures provided in the literature were measured worldwide(Kelley et al., 1999) including various locations across Japan(Momoshima et al., 1997; Muramatsu et al., 2003; Ohtsuka et al., 2004; Zhang et al., 2010). As the range of these Pu signatures is relatively wide (Table S3), there is a need to refine the global fallout signatures for this specific sampling location in the Fukushima Prefecture. In this study, the measurements conducted on the bottom sediment sample layer in the core and on the soil samples collected before the accident were used to provide the local signatures of the global fallout.

Unlike Pu, U is also naturally present in the environment with two primordial isotopes ($^{238}U$ and $^{235}U$) and one radiogenic isotope ($^{234}U$) originating from the $^{238}U$-decay. Moreover, these isotopes are relatively abundant in soils and sediment, with the U concentration being 6 to 9 orders of magnitude higher than that of Pu(Bu et al., 2017). On the contrary, the $^{236}U$ isotope has an extremely low abundance in natural-occurring U present in environmental samples ($<10^{-13}$). However, $^{236}U$ is also produced in significant quantities in nuclear reactors (by the capture of a neutron by the fissile nuclide $^{235}U$), which may result in $^{236}U/^{238}U$ ratios locally higher in those samples collected in the close vicinity of some nuclear installations. For the U ratio representative of the FDNPP signature, only Nishihara *et al.*(2012) estimated the $^{236}U/^{238}U$ in the nuclear fuel ratio at the time of the accident, being $(3.20 - 3.71) \times 10^{-3}$ (mean $(3.42 \pm 0.52) \times 10^{-3}$, $2\sigma$). Nevertheless, the main contribution of $^{236}U$ in soils is, as for Pu isotopes, the global fallout associated with the nuclear weapon atmospheric tests.

The representative $^{236}U/^{238}U$ ratios for the global fallout signature in Japan were previously measured in a soil core (n=3) sampled in the Ishikawa Prefecture(Sakaguchi et al., 2009) ($1.85\times10^{-8} - 1.09\times10^{-7}$, mean $(5.31\pm 0.12)\times10^{-8}$, $2\sigma$). However, Schneider *et al.*(2017) recently determined even lower $^{236}U/^{238}U$ ratios in the range of $10^{-9}$ in soil samples collected at various locations within the exclusion zone nearby the FDNPP, and reported this signature as that of 'undisturbed uranium'. Currently, this ratio remains poorly constrained with values varying between $10^{-10}$ and $10^{-7}$.

The potential occurrence of U contamination following the FDNPP accident in the environment has been examined in very few studies(Sakaguchi et al., 2014; Schneider et al., 2017; Shinonaga et al., 2014; Yang et al., 2016) (See Table S4). Most of these samples reported $^{236}U/^{238}U$ ratios between $10^{-8}$ and $10^{-7}$, which suggests a global fallout origin(Sakaguchi et al., 2010). Shinonaga *et al.*(2014) measured ratios of $10^{-6}$ in aerosol filter samples collected at 120 km from the FDNPP shortly after the accident. However, as early as in April 2011 U ratios measured in aerosols collected at the same location returned to the global fallout level. These results suggested that U was only released in trace amounts during the FDNPP accident.

Accordingly, in the current research, the U isotope compositions were only analysed in the sediment core, as the soil erosion and sediment transport processes are known to be selective and to mobilize preferentially the finest and most contaminated particles(Evrard et al., 2015; Laceby et al., 2017). Furthermore, $^{236}U$ concentrations in the soil samples collected before and after the accident would likely be too low to be detectable by ICP-MS with the chemical processes followed in this study.

## Quantifying source contributions

The proportions of each source of Pu were determined using a binary mixing model(Kelley et al., 1999). To this end, the isotopic abundance of $^{241}Pu$ in each source term and in each sediment sample and each soil sample collected after the accident was calculated. $^{241}Pu$ abundance was used owing to its relatively short half-life resulting in this isotope providing the best discrimination between emissions from the global fallout or the FDNPP accident. Atomic abundance of each term $Ab(^{241}Pu)_{sample}$, $Ab(^{241}Pu)_{GF}$ or $Ab(^{241}Pu)_{FDNPP}$ is given in Equation 1:

$$Ab(^{241}Pu)_i = \frac{(^{241}Pu/^{239}Pu)_i}{1+(^{240}Pu/^{239}Pu)_i+(^{241}Pu/^{239}Pu)_i+(^{242}Pu/^{239}Pu)_i} \quad (1)$$

where $i$ stands for "sample" or "GF" or "FDNPP".

Abundance for FDNPP source $Ab(^{241}Pu)_{FDNPP}$ as estimated at $(1.15\pm0.12)\times10^{-2}$ based on results published by Nishihara *et al.*(2012), Kirchner *et al.*(2012) and Schwantes *et al.*(2012). Other end-member abundances were derived from our measurements. Then, the proportions of each source term were deduced using a mixing equation with two sources (Equation 2):

$$Ab(^{241}Pu)_{FDNPP}\times X_{FDNPP}+Ab(^{241}Pu)_{GF}\times(1-X_{FDNPP})= Ab(^{241}Pu)_{sample} \quad (2)$$

It is important to note that $X_{FDNPP}$ is defined based on the total plutonium counting rates (equation 3):

$$X_{FDNPP} = \frac{\left(^{239}Pu + ^{240}Pu + ^{241}Pu + ^{242}Pu\right)_{FDNPP}}{\left(^{239}Pu + ^{240}Pu + ^{241}Pu + ^{242}Pu\right)_{sample}} \quad (3)$$

These proportions, based on the atomic ratio, were converted into mass proportions to determine the Pu concentrations originating from the FDNPP relative to those derived from the global fallout.

Although no source contribution could be modelled for U, theoretical $^{236}U$ concentrations released from the FDNPP were estimated based on the results of plutonium concentrations found in the samples analysed in the current research. First, the corresponding theoretical $^{236}U/(^{239}Pu+^{240}Pu+^{241}Pu+^{242}Pu)$ isotope ratios were estimated to be 0.46 ± 0.12 (2σ)(Nishihara et al., 2012), based on literature data. Then, the concentration of FDNPP-derived $^{236}U$ ($^{236}U_{FDNPP}$) was estimated based on the estimations of the FDNPP-derived Pu concentrations found in the soil samples, and compared with the global fallout derived $^{236}U$ concentration.

## Results and discussion

### Refining the Pu global fallout signature in soils and sediment of the Fukushima Prefecture

In the sediment core collected in the Hayama Lake, the $^{240}Pu/^{239}Pu$, $^{241}Pu/^{239}Pu$ and the $^{242}Pu/^{239}Pu$ isotope ratios measured in the bottom layer (31 cm, MD7) were within the range of values for the global fallout reported in the literature. Accordingly, it is assumed that these actinides in the bottom layer of the core were likely supplied by the global fallout.

In the soil samples collected before the accident, no Pu was detected in the SBA4 sample (Table 1). Pu isotope ratios found in other samples are surprisingly higher and more heterogeneous than the

values previously published in the literature, particularly for the $^{241}Pu/^{239}Pu$ ratio, which ranged from 0.0023 to 0.0117 (mean 0.0061± 0.0010, 2 σ). The relative proximity of the sites where Chinese nuclear weapons were tested between 1964 and 1980 may have resulted in these high values. However, the maximum $^{241}Pu/^{239+240}Pu$ activity ratio measured in the current study is 61 ± 12 (SBA2, decay-corrected to the date of the main test on November 17, 1976), which is higher than that measured in the Chinese test debris (11 according to Zhang *et al.*,(2010) and Hirose *et al.*(2001)). More research is required to investigate these high pre-FDNPP accident plutonium isotope ratio values and their heterogeneity.

Table 1: $^{137}Cs$ activities and Pu isotope ratios measured in the soil samples collected before the accident. $^{241}Pu/^{239}Pu$ is decay-corrected to March 15, 2011. Uncertainties are extended with a coverage factor of 2.

| Sample label | $^{137}Cs$ (Bq/kg) | $^{240}Pu/^{239}Pu$ | $^{241}Pu/^{239}Pu$ | $^{242}Pu/^{239}Pu$ | Pu concentration (fg/g) |
|---|---|---|---|---|---|
| SBA1 | 5.0 ± 1.4 | 0.182 ± 0.012 | 0.0044 ± 0.0017 | 0.0056 ± 0.0010 | 48.1 ± 5.9 |
| SBA2 | 3.7 ± 0.8 | 0.179 ± 0.007 | 0.0117 ± 0.0023 | 0.0071 ± 0.0006 | 29.5 ± 1.1 |
| SBA3 | 3.1 ± 1.2 | 0.179 ± 0.013 | 0.0023 ± 0.0005 | 0.0052 ± 0.0013 | 22.4 ± 1.8 |
| SBA4 | < 2.8 | - | - | - | < 0.5 |

To model the source contributions of Pu in the samples, the Pu isotope ratios characterising the local signature of the global fallout in the Mano River catchment was calculated based on those results obtained for samples exposed only to the global fallout: the pre-accident soil samples (SBA1, SBA2 and SBA3) and the bottom layer of the sediment core (MD7). Accordingly, the mean plutonium isotope ratios characterising the global fallout signature in the study area are: $^{240}Pu/^{239}Pu = 0.180 \pm 0.010$; $^{241}Pu/^{239}Pu = 0.0052 \pm 0.0017$ and $^{242}Pu/^{239}Pu = 0.0054 \pm 0.0022$ (uncertainties are extended with a coverage factor of 2.)

330 **Initial surface deposition of plutonium in the Mano catchment**

331

332 Pu isotope ratios were measured in eight soil samples collected in the catchment after the accident
333 (Table 2). Results showed that Pu isotope ratios remained generally close to the global fallout
334 signature: the atomic proportions of Pu from the FDNPP in these soils were estimated to be lower
335 than 7 % (see Table 2, Table S5). Sample FMS243 provides an exception to this rule, as it contained
336 more than 40 % of Pu from the power plant. On the contrary, low isotope ratios were measured in
337 sample FMS113, in particular the $^{240}Pu/^{239}Pu$ isotope ratio (0.160 ± 0.011). The relevance of this value
338 is confirmed by the measurement of similar ratios in Japanese soils: Muramatsu *et al.*(2003)
339 observed a ratio of 0.155 ± 0.003 in a forest soil sample collected before 2002, and Zheng *et*
340 *al.*(2012b) found a ratio of 0.144 ± 0.006 in a soil sample collected in 2011 at 32 km from the FDNPP.
341 Moreover, no correlation ($p$<0.001) could be observed between $^{137}Cs$ activities and Pu isotope ratios
342 in these samples. This confirms that Pu deposition on soils was locally heterogeneous(Salbu, 2011 ;
343 Schneider et al., 2013). It may also reflect the occurrence of different processes of aerial transport of
344 radiocesium and Pu from the FDNPP to the study area.

345 Table 2: $^{137}$Cs activities and Pu isotope ratios measured in the soil samples collected after the FDNPP accident across the Mano River catchment. Uncertainties are extended

346 with a coverage factor of 2.

| Sample label | $^{137}$Cs (kBq/kg) | $^{240}$Pu/$^{239}$Pu | $^{241}$Pu/$^{239}$Pu | $^{242}$Pu/$^{239}$Pu | Pu concentration (fg/g) | Fraction of Pu from FDNPP (%) |
|---|---|---|---|---|---|---|
| FMS059A | 18.70 ± 0.94 | 0.177 ± 0.014 | 0.0033 ± 0.0017 | 0.0048 ± 0.0019 | 112.1 ± 6.1 | 1.4 ± 1.2 |
| FMS060A | 30.59 ± 1.50 | 0.184 ± 0.017 | 0.0075 ± 0.0045 | 0.0059 ± 0.0016 | 45.8 ± 3.9 | 4.4 ± 3.3 |
| FMS243 | 19.40 ± 0.97 | 0.285 ± 0.049 | 0.0666 ± 0.0178 | 0.0488 ± 0.0029 | 75.6 ± 9.6 | 40.6 ± 11.4 |
| FMS244 | 65.72 ± 3.30 | 0.188 ± 0.019 | 0.0069 ± 0.0009 | 0.0057 ± 0.0010 | 78.4 ± 6.0 | 3.9 ± 0.8 |
| FMS113 | 13.37 ± 0.67 | 0.160 ± 0.011 | 0.0058 ± 0.0018 | 0.0075 ± 0.0029 | 61.0 ± 6.2 | 3.2 ± 1.4 |
| FMS121 | 0.19 ± 0.01 | 0.184 ± 0.011 | 0.0027 ± 0.0017 | 0.0057 ± 0.0007 | 48.0 ± 3.5 | 0.9 ± 1.3 |
| FMS124 | 3.28 ± 0.16 | 0.197 ± 0.013 | 0.0113 ± 0.0062 | 0.0116 ± 0.0008 | 67.4 ± 5.4 | 7.0 ± 4.5 |
| FMS126 | 0.84 ± 0.04 | 0.187 ± 0.016 | 0.0094 ± 0.0010 | 0.0124 ± 0.0022 | 26.1 ± 2.0 | 5.7 ± 1.0 |

347

348

**Temporal variations of radiocesium in the sediment core**

The $^{137}Cs$ activities in the sediment core demonstrated that the lowest activity (mean = 0.58 ± 0.03 Bq/g) was found in the bottom of the core (at 31 – 37 cm depth). The maximum activity was observed at 11 – 12 cm (40.24 ± 2.01 Bq/g) before decreasing in the upper part of the core (at 0-7 cm depth) to a mean of 16.96 ± 0.85 Bq/g (Table 3). The maximum of activity corresponds to the deposition of strongly contaminated sediment in the reservoir shortly after the FDNPP accident. This increase of the activity likely reflects the radiocesium wash-off and migration phase during the six first months that followed the FDNPP accident(Huon et al., 2018).

Table 3: $^{137}$Cs activities and Pu isotope ratios and Pu concentrations measured in the Mano Dam sediment core. Uncertainties are extended with a coverage factor of 2.

| Sample depth (cm) | Sample ID | $^{137}$Cs (kBq/kg) | $^{240}$Pu/$^{239}$Pu | $^{241}$Pu/$^{239}$Pu | $^{242}$Pu/$^{239}$Pu | Pu concentration (fg/g) |
|---|---|---|---|---|---|---|
| 0-1 | MD1 | 19.67 ± 0.98 | 0.180 ± 0.002 | 0.0038 ± 0.0007 | 0.0043 ± 0.0003 | 155.5 ± 11.3 |
| 1-2 | | 18.27 ± 0.91 | | | | |
| 2-3 | - | 17.77 ± 0.89 | - | - | - | - |
| 3-4 | - | 15.99 ± 0.80 | - | - | - | - |
| 4-5 | - | 15.39 ± 0.77 | - | - | - | - |
| 5-6 | MD2 | 15.31 ± 0.77 | 0.172 ± 0.002 | 0.0045 ± 0.0008 | 0.0060 ± 0.0004 | 233.8 ± 21.0 |
| 6-7 | | 16.35 ± 0.82 | | | | |
| 7-8 | MD3 | 21.06 ± 1.05 | 0.174 ± 0.002 | 0.0033 ± 0.0007 | 0.0042 ± 0.0003 | 170.3 ± 25.3 |
| 8-9 | | 26.55 ± 1.33 | | | | |
| 9-10 | MD4 | 31.76 ± 1.59 | 0.184 ± 0.002 | 0.0060 ± 0.0012 | 0.0054 ± 0.0005 | 123.0 ± 12.6 |
| 10-11 | | 31.23 ± 1.56 | | | | |
| 11-12 | MD5 | 40.24 ± 2.01 | 0.182 ± 0.002 | 0.0080 ± 0.0011 | 0.0062 ± 0.0003 | 77.5 ± 12.1 |
| 12-13 | | 31.43 ± 1.57 | | | | |
| 13-14 | - | 15.22 ± 0.76 | - | - | - | - |
| 14-15 | - | 7.91 ± 0.40 | - | - | - | - |
| 15-17 | MD6 | 2.64 ± 0.13 | 0.159 ± 0.001 | 0.0015 ± 0.0004 | 0.0034 ± 0.0005 | 209.1 ± 32.5 |
| 17-19 | | 0.99 ± 0.05 | | | | |
| 19-21 | - | 0.81 ± 0.04 | - | - | - | - |
| 21-23 | - | 0.88 ± 0.04 | - | - | - | - |
| 23-25 | - | 0.77 ± 0.04 | - | - | - | - |
| 25-28 | - | 0.48 ± 0.02 | - | - | - | - |
| 28-31 | - | 0.24 ± 0.01 | - | - | - | - |
| 31-34 | MD7 | 0.29 ± 0.01 | 0.175 ± 0.002 | 0.0022 ± 0.0008 | 0.0037 ± 0.0003 | 84.1 ± 11.4 |
| 34-37 | | 0.21 ± 0.01 | | | | |

**Change of plutonium isotopic composition with depth**

The evolution of the Pu isotopic composition with depth showed a similar pattern as $^{137}$Cs activity (see Table 3 and Figure 2). All isotope ratios ($^{240}$Pu/$^{239}$Pu, $^{241}$Pu/$^{239}$Pu and $^{242}$Pu/$^{239}$Pu) had a low value at the bottom of the core. Then, all ratios increased up to maximum values found at 11-12 cm depth, which corresponds to the peak in the $^{137}$Cs activity. The variations on the sediment core with depth clearly

reflect changes in the origin of Pu(Evrard et al., 2014; Jaegler et al., 2018), ranging between the global fallout signature and the FDNPP signature (see Figure S1), with the exception of the $^{240}Pu/^{239}Pu$ isotope ratio measured in one sample (see below).

For $^{240}Pu/^{239}Pu$ ratios, all values remained in the range of the global fallout (Figure 2) although the highest ratios corresponded to the maximum $^{137}Cs$ activity observed in the 11-12 cm depth layer. A surprisingly low ratio value of 0.159±0.001 was found in the layer MD6 (15 – 19cm depth). Similar ratios lower than or equal to 0.16 were previously reported in Japan: Muramatsu *et al.*(2003) and Zheng *et al.*(2012b), and Evrard *et al.*(2014), who measured a ratio of 0.150 ± 0.005 in a sediment sample collected in 2012. For those $^{241}Pu/^{239}Pu$ atom ratios, all isotope ratios measured in sediment samples collected between 0 and 10 cm depth in the core were significantly higher than the upper limit of the global fallout signature updated in the current study, showing a clear influence of the FDNPP inputs. A good correlation was observed between this ratio in particular and the $^{137}Cs$ activities (correlation coefficient of 0.90, $p$-value < 0.001). Finally, when examining $^{242}Pu/^{239}Pu$ values, they were slightly higher than the upper limit of the global fallout, demonstrating a very low, although clear, impact of the FDNPP fallout.

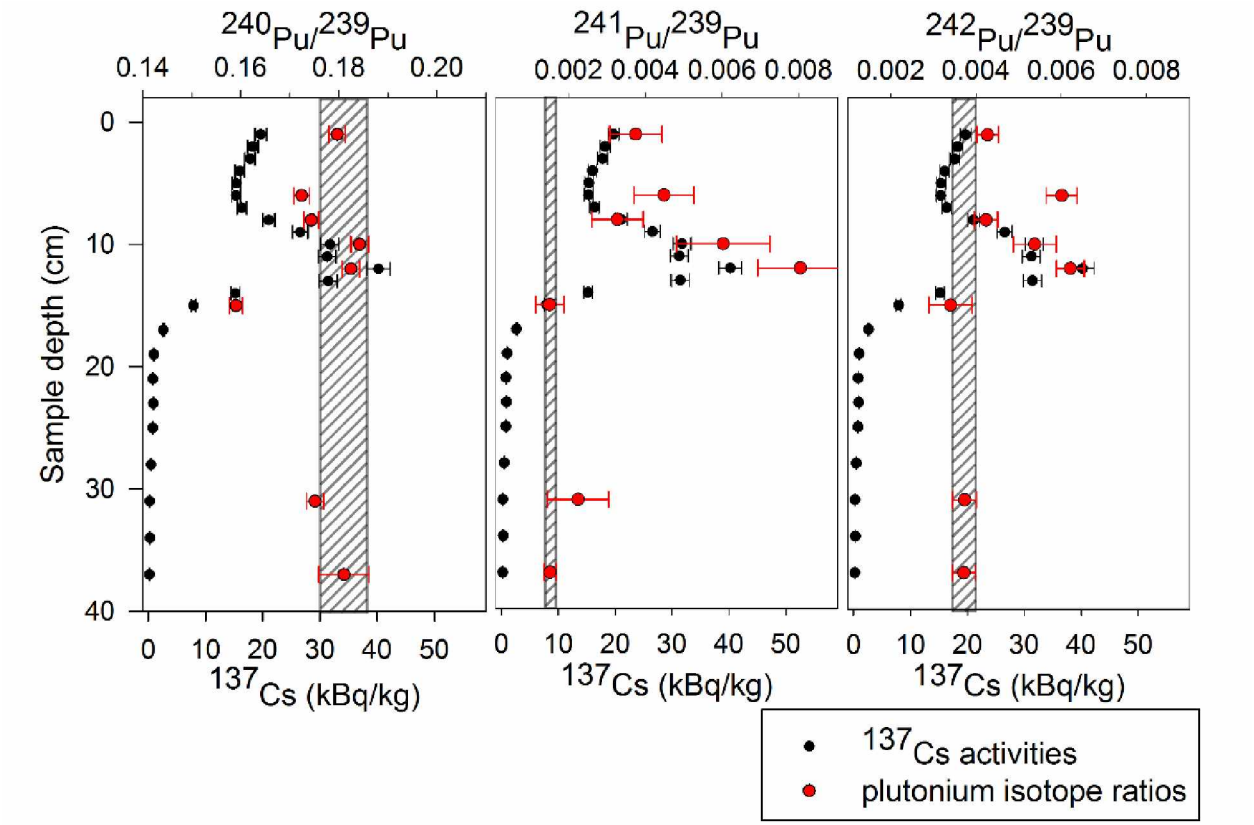


Figure 2: Evolution of $^{137}Cs$ activities (black dots), $^{240}Pu/^{239}Pu$, $^{241}Pu/^{239}Pu$ and $^{242}Pu/^{239}Pu$ atom ratios (red dots) with depth in the Mano Dam sediment core. The dashed zones provide the corresponding range of values reported for the global fallout, according to the literature(Kelley et al., 1999; Momoshima et al., 1997; Muramatsu et al., 2003; Ohtsuka et al., 2004; Zhang et al., 2010). Uncertainties are extended with a coverage factor of 2.

**Sources of plutonium in the sediment core**

The maximum isotope ratio (MD5) corresponded to a maximum FDNPP atomic contribution estimated to be 4.3 ± 1.0 %. The measurement conducted on the deeper MD6 sediment layer showed the absence of contribution from FDNPP (0.0 ± 0.7 %). This result suggested that the migration of Pu with depth in the sediment profile was negligible.

Although detectable, the release of Pu from the FDNPP remained low in the sediment accumulated in the Mano Dam (Table S6). Accordingly, the Pu detected in the sediment samples was mainly supplied by the global fallout.

The shape of the three Pu isotopes profiles shows the occurrence of large variations, which were not observed for the $^{137}Cs$ activity profile. No correlation ($p$=0.015) was found between $^{137}Cs$ and Pu concentrations, as the main source that supplied these two radionuclides strongly differed: $^{137}Cs$ was mainly supplied by the FDNPP releases, whereas Pu mainly originated from the global fallout. The variations of Pu in the core likely reflect the heterogeneity of the Pu isotope ratios derived from the global fallout as the global fallout Pu concentration was shown to be strongly heterogeneous(Kelley et al., 1999) due to the particulate form of deposition(Salbu, 2011).

**Evolution of the $^{236}U$ isotopic signature in the sediment core**

Data obtained with the two analytical methodologies were in very good agreement ($R^2$ = 0.99, slope of linear regression = 0.99) (Figure S2). The measured $^{236}U/^{238}U$ isotope ratios ranged between $(7.33 \pm 2.20) \times 10^{-9}$ and $(2.70 \pm 0.37) \times 10^{-8}$ (see Figure 3). These ratios were similar to the global fallout values ($10^{-10}$ - $10^{-7}$)(Sakaguchi et al., 2009; Schneider et al., 2017), relative to the FDNPP range ($(3.42 \pm 0.52) \times 10^{-3}$)(Nishihara et al., 2012). The increase in $^{236}U/^{238}U$ values observed in the upper section of the core is difficult to interpret because it may either reflect a slight impact of FDNPP derived U releases or a local heterogeneity of the U concentration in the environment. Nevertheless, it may be deduced from these measurements that the isotopic signature of U in these samples remained well within the range of global fallout so that the potential fallout from the FDNPP is not detectable in these samples. A part of U released from the FDNPP may also have been slowly incorporated into the bottom

sediment, which could explain the slight increase of the $^{236}U/^{238}U$ isotope ratio observed in the upper part of the core and the absence of a peak similar to that recorded for radiocesium and Pu. Moreover, the geochemical behaviour of U may be different from that of radiocesium as it is likely contained in $UO_2$ microparticles from the nuclear fuel in association with Pu impurities. The absence of the detection of FDNPP –derived U suggested that the concentrations in actinide released from the power plant were lower than those already prevailing in the environment before the accident.

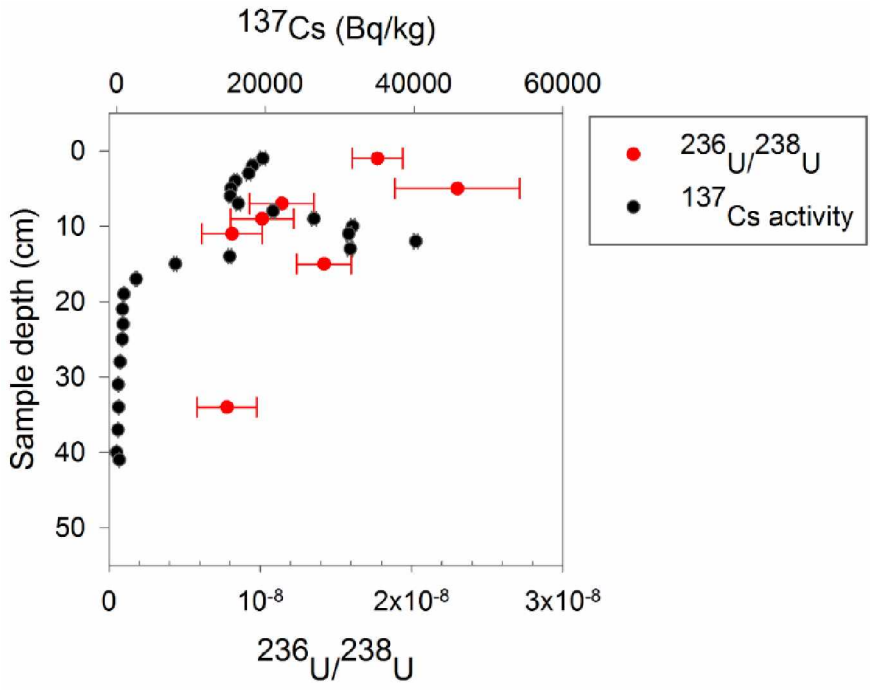


Figure 3: Evolution of the mean $^{236}U/^{238}U$ atom ratios (red dots) and $^{137}Cs$ activities (black dots) with depth in the Mano Dam sediment core. Uncertainties are extended with a coverage factor of 2. The uranium global fallout signature ($10^{-10}$ – $10^{-7}$) falls beyond the range of the X-axis.

**Detectability of uranium releases from the FDNPP**

Although it was not possible to calculate the U source contributions as it was done for Pu, theoretical FDNPP-derived $^{236}U$ concentrations ($^{236}U_{FDNPP}$) in the samples analysed in the current study were estimated, based on the $^{236}U/Pu$ =(0.46±0.12) ratio determined from the literature data(Nishihara et al., 2012). The maximum FDNPP-derived Pu concentration in soil samples analysed here reached 30.7±9.4 fg/g (Table S5). Accordingly, the theoretical $^{236}U$ concentration from the FDNPP was estimated to a maximum of 14.1 ± 5.6 fg/g. Assuming a natural U concentration in Japanese soils of 1.9±1.2 µg/g(Yoshida et al., 1998; Yoshida et al., 2000), the estimation of the theoretical $^{236}U_{FDNPP}/^{238}U$ (i.e. the potential impact of the FDNPP releases on the $^{236}U/^{238}U$ measured in the samples) was (7.6±5.2) × $10^{-9}$. This theoretical calculation demonstrates that the occurrence of FDNPP-originating fallout is not detectable in the analysed samples, because there is no significant difference between the $^{236}U_{FDNPP}$ /$^{238}U$ ratio in these sediment samples and the $^{236}U/^{238}U$ isotope ratio associated with the very heterogeneous global fallout signal ($10^{-10}$ – $10^{-7}$).

Similar calculations were performed to estimate the theoretical $^{236}U$ concentrations in the sediment core, based on the FDNPP-derived Pu measurements in these samples. The resulting concentration amounts to 1.7 fg/g, which demonstrates that the FDNPP-originating U fallout did not reach the region of interest located at ~40 km from the power plant. Nevertheless, the potential occurrence of U emissions by the FDNPP accident needs further investigations. In particular, similar analyses should be performed in more contaminated areas such as in sediment accumulated in lakes located closer to the FDNPP, where uranium may have been released in larger quantities.

## Acknowledgements:

The collection and the analysis of the sediment samples were funded by the TOFU (ANR-11-JAPN-001) and the AMORAD (ANR-11-RSNR-0002) projects, funded by the French National Research Agency (ANR, *Agence Nationale de la Recherche*). Hugo Jaegler received a PhD fellowship from the French Atomic Energy Commission (CEA, Commissariat à l'Energie Atomique et aux Energies Alternatives). The authors are grateful to the Fukushima Agricultural Technology Centre for providing the soil samples collected before the FDNPP accident. The authors declare no competing financial interest

# References


Bu, W., Zheng, J., Ketterer, M.E., Hu, S., Uchida, S., Wang, X. (2017) Development and application of mass spectrometric techniques for the ultra-trace determination of $^{236}U$ in environmental samples-A review. Analytica Chimica Acta.

Buesseler, K., Dai, M., Aoyama, M., Benitez-Nelson, C., Charmasson, S., Higley, K., Maderich, V., Masque, P., Oughton, D., Smith, J.N. (2016) Fukushima Daiichi-Derived Radionuclides in the Ocean: Transport, Fate, and Impacts. Annual Review of Marine Science.

Cao, L., Ishii, N., Zheng, J., Kagami, M., Pan, S., Tagami, K., Uchida, S. (2017) Vertical distributions of Pu and radiocesium isotopes in sediments from Lake Inba after the Fukushima Daiichi Nuclear Power Plant accident: Source identification and accumulation. Applied Geochemistry 78, 287-294.

Cao, L., Zheng, J., Tsukada, H., Pan, S., Wang, Z., Tagami, K., Uchida, S. (2016) Simultaneous determination of radiocesium ((135)Cs, (137)Cs) and plutonium ((239)Pu, (240)Pu) isotopes in river suspended particles by ICP-MS/MS and SF-ICP-MS. Talanta 159, 55-63.

Chartin, C., Evrard, O., Laceby, J.P., Onda, Y., Ottlé, C., Lefèvre, I., Cerdan, O. (2017) The impact of typhoons on sediment connectivity: lessons learnt from contaminated coastal catchments of the Fukushima Prefecture (Japan). Earth Surface Processes and Landforms 42, 306-317.

Chartin, C., Evrard, O., Onda, Y., Patin, J., Lefèvre, I., Ottlé, C., Ayrault, S., Lepage, H., Bonté, P. (2013) Tracking the early dispersion of contaminated sediment along rivers draining the Fukushima radioactive pollution plume. Anthropocene 1, 23-34.

Evrard, O., Laceby, J.P., Lepage, H., Onda, Y., Cerdan, O., Ayrault, S. (2015) Radiocesium transfer from hillslopes to the Pacific Ocean after the Fukushima Nuclear Power Plant accident: A review. Journal of Environmental Radioactivity 148, 92-110.

Evrard, O., Laceby, J.P., Onda, Y., Wakiyama, Y., Jaegler, H., Lefèvre, I. (2016) Quantifying the dilution of the radiocesium contamination in Fukushima coastal river sediment (2011–2015). Scientific Reports 6, 34828.

Evrard, O., Pointurier, F., Onda, Y., Chartin, C., Hubert, A., Lepage, H., Pottin, A.C., Lefevre, I., Bonte, P., Laceby, J.P., Ayrault, S. (2014) Novel insights into Fukushima nuclear accident from isotopic evidence of plutonium spread along coastal rivers. Environmental Science & Technology 48, 9334-9340.

Fukushima, T., Arai, H. (2014) Radiocesium contamination of lake sediments and fish following the Fukushima nuclear accident and their partition coefficient. Inland Waters 4, 2014 - 2214.

Hirose, K., Igarashi, Y., Aoyama, M., Miyao, T., (2001) Long-term trends of plutonium fallout observed in Japan, in: Kudo, A. (Ed.), Radioactivity in the Environment. Elsevier, pp. 251-266.

Huon, S., Hayashi, S., Laceby, J.P., Tsuji, H., Onda, Y., Evrard, O. (2018) Source dynamics of radiocesium-contaminated particulate matter deposited in an agricultural water reservoir after the Fukushima nuclear accident. Science of The Total Environment 612, 1079-1090.

Jaegler, H., Pointurier, F., Onda, Y., Hubert, A., Laceby, J.P., Cirella, M., Evrard, O. (2018) Plutonium isotopic signatures in soils and their variation (2011-2014) in sediment transiting a coastal river in the Fukushima Prefecture, Japan. Environmental Pollution 240, 167-176.

Kelley, J.M., Bond, L.A., Beasley, T.M. (1999) Global distribution of Pu isotopes and $^{237}Np$. Science of The Total Environment 237–238, 483-500.

Kirchner, G., Bossew, P., De Cort, M. (2012) Radioactivity from Fukushima Dai-ichi in air over Europe; part 2: what can it tell us about the accident? Journal of Environmental Radioactivity 114, 35-40.

Kitamura, A., Kurikami, H., Sakuma, K., Malins, A., Okumura, M., Machida, M., Mori, K., Tada, K., Tawara, Y., Kobayashi, T., Yoshida, T., Tosaka, H. (2016) Redistribution and export of contaminated sediment

within eastern Fukushima Prefecture due to typhoon flooding. Earth Surface Processes and Landforms 41, 1708-1726.
Kitamura, A., Yamaguchi, M., Kurikami, H., Yui, M., Onishi, Y. (2014) Predicting sediment and cesium-137 discharge from catchments in eastern Fukushima. Anthropocene 5, 22-31.
Laceby, J.P., Evrard, O., Smith, H.G., Blake, W.H., Olley, J.M., Minella, J.P.G., Owens, P.N. (2017) The challenges and opportunities of addressing particle size effects in sediment source fingerprinting: A review. Earth-Science Reviews 169, 85-103.
Laceby, J.P., Huon, S., Onda, Y., Vaury, V., Evrard, O. (2016) Do forests represent a long-term source of contaminated particulate matter in the Fukushima Prefecture? Journal of Environmental Management 183, 742-753.
Lee, S.H., La Rosa, J., Gastaud, J., Povinec, P.P. (2005) The development of sequential separation methods for the analysis of actinides in sediments and biological materials using anion-exchange resins and extraction chromatography. Journal of Radioanalytical and Nuclear Chemistry 263, 419-425.
Lepage, H., Laceby, J.P., Bonté, P., Joron, J.-L., Onda, Y., Lefèvre, I., Ayrault, S., Evrard, O. (2016) Investigating the source of radiocesium contaminated sediment in two Fukushima coastal catchments with sediment tracing techniques. Anthropocene.
Matsuda, K., Takagi, K., Tomiya, A., Enomoto, M., Tsuboi, J.-i., Kaeriyama, H., Ambe, D., Fujimoto, K., Ono, T., Uchida, K., Morita, T., Yamamoto, S. (2015) Comparison of radioactive cesium contamination of lake water, bottom sediment, plankton, and freshwater fish among lakes of Fukushima Prefecture, Japan after the Fukushima fallout. Fisheries Science 81, 737-747.
Momoshima, N., Kakiuchi, H., Maeda, Y., Hirai, E., Ono, T. (1997) Identification of the contamination source of plutonium in environmental samples with isotopic ratios determined by inductively coupled plasma mass spectrometry and alpha-spectrometry. Journal of Radioanalytical and Nuclear Chemistry 221, 213-217.
Muramatsu, Y., Yoshida, S., Tanaka, A. (2003) Determination of Pu concentration and its isotope ratio in Japanese soils by HR-ICP-MS. Journal of Radioanalytical and Nuclear Chemistry 255, 477-480.
Nishihara, K., Iwamoto, H., Suyama, K. (2012) Estimation of fuel compositions in Fukushima-Daiichi nuclear power plant. JAEA-Data/Code 2012, http://jolissrch-inter.tokai-sc.jaea.go.jp/pdfdata/JAEA-Data-Code-2012-018.pdf (2012)(Date of access: 29/02/2016).
Ohtsuka, Y., T., I., Kakiuchi, H., Y., T., Hisamatsu, S., J., I. (2004) Evalutation of 239+240Pu, 137Cs and natural 210Pb fallout in agricultural upland fields in Rokkasho, Japan. Journal of Radioanalytical and Nuclear Chemistry 261, 625-630.
Sakaguchi, A., Kawai, H., Steier, P., Imanaka, T., Hoshi, M., Endo, I., Zhumadilov, K., M., Y. (2010) Feasibility of using 236U to reconstruct close-in fallout deposition from the hiroshima atomic bomb. Science of The Total Environment 408, 5392 - 5398.
Sakaguchi, A., Kawai, K., Steier, P., Quinto, F., Mino, K., Tomita, J., Hoshi, M., Whitehead, N., Yamamoto, M. (2009) First results on $^{236}$U levels in global fallout. Science of The Total Environment 407, 4238-4242.
Sakaguchi, A., Steier, P., Takahashi, Y., Yamamoto, M. (2014) Isotopic Compositions of $^{236}$U and Pu Isotopes in "Black Substances" Collected from Roadsides in Fukushima Prefecture: Fallout from the Fukushima Dai-ichi Nuclear Power Plant Accident. Environmental Science & Technology 48, 3691-3697.
Salbu, B. (2011) Radionuclides released to the environment following nuclear events. Integrated Environmental Assessment and Management 7, 362-364.
Schneider, S., Bister, S., Christl, M., Hori, M., Shozugawa, K., Synal, H.-A., Steinhauser, G., Walther, C. (2017) Radionuclide pollution inside the Fukushima Daiichi exclusion zone, part 2: Forensic search for the "Forgotten" contaminants Uranium-236 and plutonium. Applied Geochemistry.
Schneider, S., Walther, C., Bister, S., Schauer, V., Christl, M., Synal, H.-A., Shozugawa, K., Steinhauser, G. (2013) Plutonium release from Fukushima Daiichi fosters the need for more detailed investigations. Scientific Reports 3.

Schwantes, J.M., Orton, C.R., Clark, R.A. (2012) Analysis of a Nuclear Accident: Fission and Activation Product Releases from the Fukushima Daiichi Nuclear Facility as Remote Indicators of Source Identification, Extent of Release, and State of Damaged Spent Nuclear Fuel. Environmental Science & Technology 46, 8621-8627.

Shinonaga, T., Steier, P., Lagos, M., Ohkura, T. (2014) Airborne Plutonium and Non-Natural Uranium from the Fukushima DNPP Found at 120 km Distance a Few Days after Reactor Hydrogen Explosions. Environmental Science & Technology 48, 3808-3814.

Tanaka, K., Iwatani, H., Sakaguchi, A., Fan, Q., Takahashi, Y. (2015) Size-dependent distribution of radiocesium in riverbed sediments and its relevance to the migration of radiocesium in river systems after the Fukushima Daiichi Nuclear Power Plant accident. Journal of Environmental Radioactivity 139, 390-397.

Tanimizu, M., Sugiyama, N., Ponzevera, E., Bayon, G. (2013) Determination of ultra low $^{236}U/^{238}U$ isotope ratios by tandem quadrupole ICP-MS. Journal of Analytical Atomic Spectrometry 28, 1372–1376.

Trémillon, B. (1965) Les séparations par les résines échangeuses d'ions. Gauthier-Villars.

Xu, C., Zhang, S., Sugiyama, Y., Ohte, N., Ho, Y.F., Fujitake, N., Kaplan, D.I., Yeager, C.M., Schwehr, K., Santschi, P.H. (2016) Role of natural organic matter on iodine and Pu distribution and mobility in environmental samples from the northwestern Fukushima Prefecture, Japan. Journal of Environmental Radioactivity 153, 156-166.

Yamada, S., Kitamura, A., Kurikami, H., Yamaguchi, M., Malins, A., Machida, M. (2015) Sediment and $^{137}Cs$ transport and accumulation in the Ogaki Dam of eastern Fukushima. Environmental Research Letters 10, 014013.

Yamamoto, M., Sakaguchi, A., Ochiai, S., Takada, T., Hamataka, K., Murakami, T., Nagao, S. (2014) Isotopic Pu, Am and Cm signatures in environmental samples contaminated by the Fukushima Dai-ichi Nuclear Power Plant accident. Journal of Environmental Radioactivity 132, 31-46.

Yamamoto, M., Takada, T., Nagao, S., Koike, T., Shimada, K., Hoshi, M., Zhumadilov, K., Shima, T., Fukuoka, M., Imanaka, T., Endo, S., Sakaguchi, A., Kimura, S. (2012) An early survey of the radioactive contamination of soil due to the Fukushima Dai-ichi Nuclear Power Plant accident, with emphasis on plutonium analysis. Geochemical Journal 46, 341-353.

Yamashiki, Y., Onda, Y., Smith, H.G., Blake, W.H., Wakahara, T., Igarashi, Y., Matsuura, Y., Yoshimura, K. (2014) Initial flux of sediment-associated radiocesium to the ocean from the largest river impacted by Fukushima Daiichi Nuclear Power Plant. Scientific Reports 4, 3714.

Yang, G., Tazoe, H., Yamada, M. (2016) Determination of $^{236}U$ in environmental samples by single extraction chromatography coupled to triple-quadrupole inductively coupled plasma-mass spectrometry. Analytica Chimica Acta.

Yoshida, S., Muramatsu, Y., Tagami, K., Uchida, S. (1998) Concentrations of lanthanide elements, Th, and U in 77 Japanese surface soils. Environment International 24, 275-286.

Yoshida, S., Muramatsu, Y., Tagami, K., Uchida, S., Ban-nai, T., Yonehara, H., Sahoo, S. (2000) Concentrations of uranium and $^{235}U/^{238}U$ ratios in soil and plant samples collected around the uranium conversion building in the JCO campus. Journal of Environmental Radioactivity 50, 121 - 172.

Zhang, Y., Zheng, J., Yamada, M., Wu, F., Igarashi, Y., Hirose, K. (2010) Characterization of Pu concentration and its isotopic composition in a reference fallout material. Science of The Total Environment 408, 1139-1144.

Zheng, J., Tagami, K., Bu, W., Uchida, S., Watanabe, Y., Kubota, Y., Fuma, S., Ihara, S. (2014) $^{135}Cs/^{137}Cs$ isotopic ratio as a new tracer of radiocesium released from the Fukushima nuclear accident. Environmental Science & Technology 48, 5433-5438.

Zheng, J., Tagami, K., Watanabe, Y., Uchida, S., Aono, T., Ishii, N., Yoshida, S., Kubota, Y., Fuma, S., Ihara, S. (2012b) Isotopic evidence of plutonium release into the environment from the Fukushima DNPP accident. Scientific Reports 2, 304.